Criteria for formation of interface dislocations in a finite thickness epilayer deposited on a substrate

Tong-Yi Zhang
Department of Mechanical Engineering, Hong Kong University of Science and Technology, Clear Water Bay, Kowloon, Hong Kong

Sanboh Lee
Department of Materials Science and Engineering, National Tsing Hua University, Hsinchu, Taiwan

L. J. Guido
Department of Electrical Engineering, Yale University, New Haven, Connecticut 06520

Chun-Hway Hsueh
Metals and Ceramics Division, Oak Ridge National Laboratory, Oak Ridge, Tennessee 37831-6068

(Received 21 September 1998; accepted for publication 16 February 1999)

The critical epilayer thickness for the formation of misfit dislocations at the interface between an epilayer and a substrate with a finite thickness is derived in the present study. The analysis is based on the energy approach, in which the self-energy of dislocation, the interaction energy between the dislocation and free surfaces, and the lattice mismatch energy of substrate and epilayer are calculated. To satisfy the free surface condition, the methodology of superposition principle and Fourier transformation are used in analyzing the stress field due to the interface dislocation. The critical epilayer thickness is compared with those reported in the literature. © *1999 American Institute of Physics.* [S0021-8979(99)06710-9]

I. INTRODUCTION

Advances in semiconductor device technology and high temperature superconducting films rely on the ability to deposit a single-crystal thin film epitaxially on a substrate. However, a lattice parameter mismatch generally exists between the epilayer and the substrate. As a result, the epilayer grows with internal stresses due to the constraint of the substrate. These internal stresses provide the driving force for the formation of mismatch dislocations at the interface between the epilayer and the substrate[1–21] that, in turn, degrades the device performance. Hence, the critical film thickness for the interface dislocation to form in the epilayer/substrate system becomes crucial in materials design. Efforts have been devoted to predict this critical thickness. Due to the complexity of the problem, the existing analyses assume the epilayer and the substrate are isotropic elastic materials and have the same elastic constants.[3,7,22] Matthews and Blakeslee (MB)[3] considered a thin epilayer on an infinitely thick substrate, analyzed the force exerted by the misfit strain and the approximate tension in the dislocation line, and used the force approach to predict the critical thickness. The MB model was subsequently improved by others[7,14,20] using the energy approach, in which the work of forming the dislocation due to the presence of internal stresses and the self-energy of the dislocation were analyzed. It has been found that the critical thickness based on an infinitely thick (i.e., noncompliant) substrate is generally too thin to fabricate devices.

To increase the critical thickness, new approaches to grow thick epilayers on compliant substrates have been proposed and preliminary results are very promising.[23–25] To generalize the MB criterion for a thin epilayer on an infinitely thick substrate to the case of a compliant substrate/epilayer system, Freund and Nix (FN)[22] estimated the free energy change in the semiconductor-on-insulator compliant substrate/epilayer system due to formation of an interface misfit dislocation. In their estimation, the thin substrate is assumed to be free standing and flat. The purpose of the present study is to refine the FN model by providing a complete analysis for the dislocation self-energy. To achieve this, the methodology of superposition principle and Fourier transformation[18–20] are adopted in analyzing the stress field due to the interface dislocation. This stress field satisfies the free surface condition. Finally, the predicted critical epilayer thickness is compared with existing solutions.

II. THEORETICAL ANALYSIS

A. Stress distribution

Like the MB and the FN models,[3,22] the present model considers that the epilayer and the substrate are isotropic elastic materials and have the same elastic constants. A schematic drawing of an epilayer with a thickness of h_f deposited on a substrate with a thickness of h_s is shown in Fig. 1. The Cartesian coordinates, x_1, x_2, and x_3, are used with the x_1 axis parallel to the in-plane interface, the x_2 axis perpendicular to the interface, and the origin located at the interface (see Fig. 1). A dislocation with a Burgers vector $b=[b_1 b_2 b_3]$ is located at the origin. In the present analysis, energies are calculated per unit length of the dislocation line or per unit depth of the epilayer/substrate system. The formation energy of the dislocation, E_f, is of primary concern. When E_f is negative, the dislocation can form spontaneously. Conversely, when E_f is positive, the interface remains coherent.

 © 1999 American Institute of Physics

Downloaded 12 Mar 2002 to 128.219.47.178. Redistribution subject to AIP license or copyright, see http://ojps.aip.org/japo/japcr.jsp

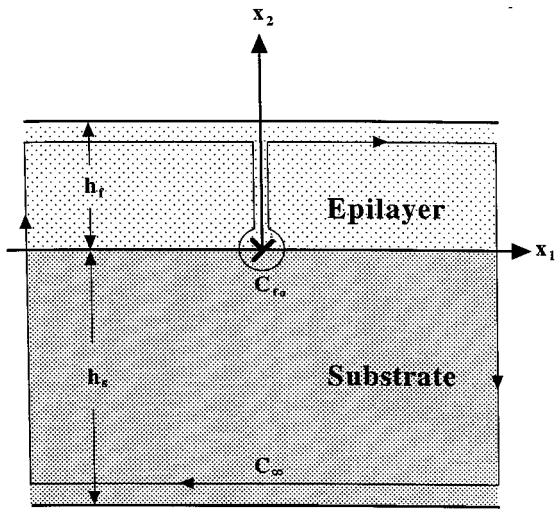

FIG. 1. Schematic diagram of a misfit dislocation located at the interface between an epilayer of thickness h_f and a substrate of thickness h_s. The coordinate system is also shown.

The formation energy of the dislocation, E_f, consists of two components: the self-energy of the dislocation, E_s, and the interaction energy between the dislocation and the mismatch strain, E_{int}, such that

$$E_f=\frac{1}{2}\int\int_{\Sigma}(\sigma_a+\sigma_m)(\epsilon_a+\epsilon_m)dx_1\,dx_2 -\frac{1}{2}\int\int_{\Sigma}\sigma_m\epsilon_m dx_1\,dx_2=E_s+E_{\text{int}},$$
$$E_s=\frac{1}{2}\int\int_{\Sigma}\sigma_a\epsilon_a dx_1\,dx_2,\quad E_{\text{int}}=\int\int_{\Sigma}\sigma_m\epsilon_a dx_1 dx_2, \tag{1}$$

where σ and ϵ are the stress and strain, and the subscripts, a and m, denote the tensor components induced by the dislocation and the mismatch, respectively. The integration domain, Σ, encloses the entire solid including the epilayer and the substrate but excluding the dislocation core because the elastic stress field induced by the dislocation is no longer valid in the core region. Application of the divergence theorem to E_s and E_{int} yields

$$E_s=\frac{1}{2}\int_S\sigma_{a,ij}n_j u_{a,i}ds,\quad E_{\text{int}}=\int_S\sigma_{m,ij}n_j u_{a,i}ds, \tag{2}$$

where the boundary of S includes two contours, C_∞ and C_{r_0}, and an arbitrary cut, as shown in Fig. 1, and n_j is a unit vector normal to the boundary. For convenience, a cut along the x_2 axis is usually made. The traction-free condition along the surfaces $x_2=h_f$ and $x_2=-h_s$, and the vanishing remote stresses of the dislocation stress field reduce Eq. (2) to

$$E_s=E_0+E_c,\quad E_0=-\frac{1}{2}\int_{r_0}^{L}\sigma_{a,ij}n_j b_i ds,$$
$$E_c=\frac{1}{2}\int_{C_{r_0}}\sigma_{a,ij}n_j u_{a,i}ds,\quad E_{\text{int}}=-\int_0^L\sigma_{m,ij}n_j b_i ds, \tag{3}$$

where L is the length of the cut, r_0 is the radius of the dislocation core, and the integration value i.e., E_c, along the core contour C_{r_0} is the core-traction contribution to the self-energy. As long as the core-traction contribution is included, the self-energy of the dislocation is independent of the cut. It is noted that the cut location changes the dislocation displacement field and hence the core-traction contribution, E_c. However, E_0 also varies with the cut location, such that the summation of E_0 and E_c becomes independent of the cut location. This issue has been discussed by Freund[14] in detail.

The stress field produced by the dislocation is derived using the superposition principle, in which four components of stress field $\sigma^{(1)}$, $\sigma^{(2)}$, $\sigma^{(3)}$, and $\sigma^{(4)}$ are considered, and Fourier transformation. First, a dislocation in an infinite domain is considered. Then, an image dislocation with respect to the free surface of the epilayer is added such that the stress field resulting from the original and the first image dislocations [i.e., $\sigma^{(1)}+\sigma^{(2)}$] satisfies the traction-free condition at $x_2=h_f$. Similarly, a second image dislocation with respect to the free surface of the substrate is added such that the stress field resulting from the original and the second image dislocations [i.e., $\sigma^{(1)}+\sigma^{(3)}$] satisfies the traction-free condition at $x_2=-h_s$. Finally, the fourth component of stress field, $\sigma^{(4)}$, calculated using Fourier transformation is added, such that the traction-free conditions at $x_2=-h_s$ and $x_2=h_f$ are satisfied, respectively, when $\sigma^{(4)}$ is combined with the stress fields due to the first and the second image dislocations. Hence, combination of the above four components satisfies the traction-free conditions at the free surfaces of epilayer and substrate.

Using the above procedures, the dislocation displacement and stress fields can be expressed as

$$u_a=u^{(1)}+u^{(2)}+u^{(3)}+u^{(4)},\quad \sigma_a=\sigma^{(1)}+\sigma^{(2)}+\sigma^{(3)}+\sigma^{(4)}. \tag{4}$$

While the stress fields due to a dislocation in an infinite domain (i.e., $\sigma^{(1)}$) and its two image dislocations (i.e., $\sigma^{(2)}$ and $\sigma^{(3)}$) can be readily obtained, determination of $\sigma^{(4)}$ is subjected to the traction-free boundary conditions, such that

$$\sigma_{i2}^{(4)}+\sigma_{i2}^{(2)}=0\,(i=1,2,3)\quad \text{at } x_2=h_f,$$
$$\sigma_{i2}^{(4)}+\sigma_{i2}^{(3)}=0\,(i=1,2,3)\quad \text{at } x_2=-h_s. \tag{5}$$

Derivation of $\sigma^{(4)}$ from Eq. (5) is complex, and the detailed derivations are given in Appendices I and II for an edge dislocation and a screw dislocation, respectively.

B. Interaction energy

The mismatch stress and strain fields in both the epilayer and the substrate have been derived in the FN model, such that the stress field σ_m produced by the mismatch is given by[22]

$$\epsilon_f=\epsilon_m^0\frac{h_s}{h_s+h_f},\quad \epsilon_s=-\epsilon_m^0\frac{h_f}{h_s+h_f},$$
$$\sigma_{11}^f=\sigma_{33}^f=M\epsilon_f,\quad \sigma_{11}^s=\sigma_{33}^s=M\epsilon_s,\quad \text{and other } \sigma_{ij}=0, \tag{6}$$

Downloaded 12 Mar 2002 to 128.219.47.178. Redistribution subject to AIP license or copyright, see http://ojps.aip.org/japo/japcr.jsp

where $M=2\mu(1+\nu)/(1-\nu)$ is the biaxial modulus, μ and ν are, respectively, the shear modulus and Poisson's ratio; $\epsilon_m^0=(a_s-a_f)/a_f$ is the unrelaxed mismatch strain, and a_s and a_f are the stress-free lattice parameters of the substrate and epilayer materials, respectively. Since the mismatch stress field is an analytic function at the dislocation core, the interaction energy can be calculated by integrating from the surface to the dislocation core. It results from completing the integration of Eq. (3) and is given by

$$E_{\text{int}}=M\epsilon_m^0 b_1\frac{h_s h_f}{h_s+h_f}. \tag{7}$$

As can be seen in Eq. (7), the product of the b_1 component of the Burgers vector and the mismatch strain must be negative to ensure a negative interaction energy which is necessary in order to form the dislocation.

C. Self-energy

When the radius of the dislocation core is much smaller than the layer thickness, substitution of the four parts of the stress field into Eq. (3), yields

$$E_0=\frac{\mu(b_1^2+b_2^2)}{4\pi(1-\nu)}\ln\left[\frac{4h_f h_s}{(h_f+2h_s)r_0}\right]+\frac{\mu b_3^2}{4\pi}\ln\left\{\left[\frac{2(h_f+h_s)}{\pi r_0}\right]\times\cos\left[\frac{\pi(h_s-h_f)}{2(h_s+h_f)}\right]\right\}-\frac{\mu(b_1^2+b_2^2)}{4\pi(1-\nu)}\left[1-\frac{2h_s}{h_f+2h_s}+\frac{2h_s^2}{(h_f+2h_s)^2}\right]+E_{0,4e}. \tag{8}$$

where $E_{0,4e}$ is induced by the fourth stress field of the edge component of the dislocation, calculated via the Fourier transformation (see Appendix 1 for details). The second term containing b_3 is the strain energy of the screw component of the dislocation (see Appendix II for details) which is the same as the exact solution for a screw dislocation in a plate with traction-free surfaces derived by Eshelby.[26] When the cut is along the x_2 axis, the core-traction contribution is given by

$$E_c=\frac{\mu}{16\pi(1-\nu)}[2(b_1^2-b_2^2)+(b_1^2+b_2^2)/(1-\nu)]. \tag{9}$$

Combining Eqs. (7), (8), and (9) leads to the formation energy for the isolated mismatch dislocation. A zero formation energy yields the critical thickness, which is determined by

$$\frac{\mu(b_1^2+b_2^2)}{4\pi(1-\nu)}\ln\left[\frac{4h_f h_s}{(h_f+2h_s)r_0}\right]+\frac{\mu b_3^2}{4\pi}\ln\left\{\left(\frac{2(h_s+h_f)}{\pi r_0}\right)\times\cos\left[\frac{\pi(h_s-h_f)}{2(h_s+h_f)}\right]\right\}-\frac{\mu(b_1^2+b_2^2)}{4\pi(1-\nu)}\times\left[1-\frac{2h_s}{h_f+2h_s}+\frac{2h_s^2}{(h_f+2h_s)^2}\right]+E_{0,4e}+E_c=M|\epsilon_m^0 b_1|\frac{h_s h_f}{h_s+h_f}. \tag{10}$$

When the substrate thickness approaches infinity, Eq. (10) is then reduced to

$$\frac{\mu}{4\pi(1-\nu)}[b_1^2+b_2^2+(1-\nu)b_3^2]\ln\left[\frac{2h_f}{r_0}\right]-\frac{\mu(b_1^2+b_2^2)}{8\pi(1-\nu)}+E_c=M|\epsilon_m^0 b_1|h_f. \tag{11}$$

Furthermore, when the core energy, E_c, is ignored, Eq. (11) becomes identical to the previous results.[7,14,20]

III. RESULTS AND DISCUSSION

In order to verify the analytic results, the contours of stress fields near an edge dislocation and a screw dislocation located at the origin on the interface are shown, respectively. Specifically, the free-surface condition is examined. The substrate thickness to epilayer thickness ratio of 3 is used in the plot to elucidate the essential trend. Comparison is then made between present and existing results.

A. Stress contours of dislocation

The contours of stress components σ_{22} and σ_{12} arising from an edge dislocation with Burgers vector $\mathbf{b}_1$ along the x_1 direction are shown in Figs. 2(a) and 2(b), respectively. It can be seen from Fig. 2(a) that the stress component σ_{22} satisfies the free-surface condition at $x_2=-h_s$ and h_f. Although contours near the dislocation are similar to those in an infinite medium, two local maxima are located near $(\pm 1.4,\ -0.7)$. The contours of shear stress, σ_{12}, shown in Fig. 2(b) deviate from those in an infinite medium near both free surfaces. The shear stress is equal to zero at both free surfaces.

The stress contours, σ_{22} and σ_{12}, arising from an edge dislocation with Burgers vector, $\mathbf{b}_2$, along the x_2 direction are shown in Figs. 3(a) and 3(b), respectively. Note that for an infinite medium, the stress fields due to an edge dislocation with Burgers vector along the x_2 direction can be obtained from those due to an edge dislocation along the x_1 direction if x_1 and x_2 are replaced by x_2 and $-x_1$, respectively. The profiles of σ_{22} are shown in Fig. 3(a). Although the shape near the edge dislocation is similar to that of an edge dislocation in an infinite medium, an additional set of enclosed contours is distributed on each side of dislocation. The value of stress σ_{22} is equal to zero at both free surfaces. The stress profiles of σ_{12} are shown in Fig. 3(b). The value of σ_{12} is equal to zero at both free surfaces, and the free-surface condition is satisfied. There exists two sets of enclosed contours located on each side of $x_1=0$.

The stress contour, σ_{23}, due to a screw dislocation with Burgers vector, $\mathbf{b}_3$, along the x_3 direction is shown in Fig. 4. The stress contours are similar to those of a screw dislocation in an infinite domain except that the circle is deformed in this case. The value of stress σ_{23} is zero at both free surfaces as expected.

B. Critical epilayer thickness

Most semiconductor materials have the diamond or the zincblende structure. The principal types of dislocations in the strong Peierls potential of semiconductor crystals are the

Downloaded 12 Mar 2002 to 128.219.47.178. Redistribution subject to AIP license or copyright, see http://ojps.aip.org/japo/japcr.jsp

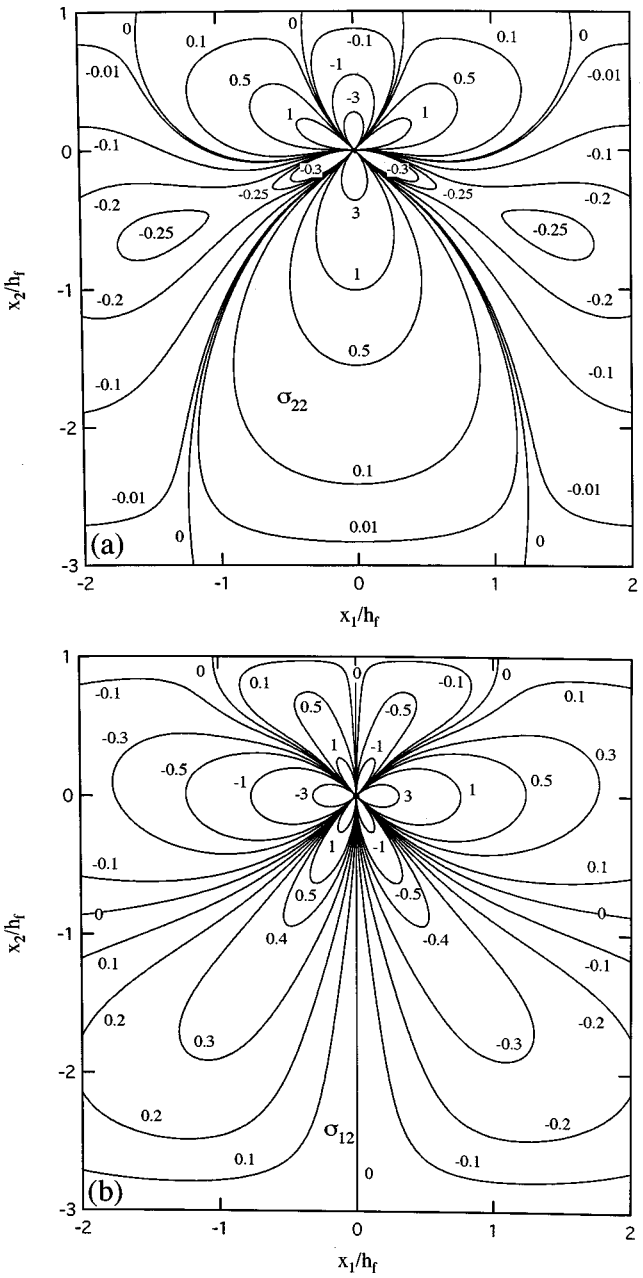

FIG. 2. Stress contours of an edge dislocation with Burgers vector $\mathbf{b}_1$ along the x_1 axis showing (a) σ_{22} and (b) σ_{12} where stresses are normalized by $\mu b_1/[2\pi(1-\nu)h_f]$.

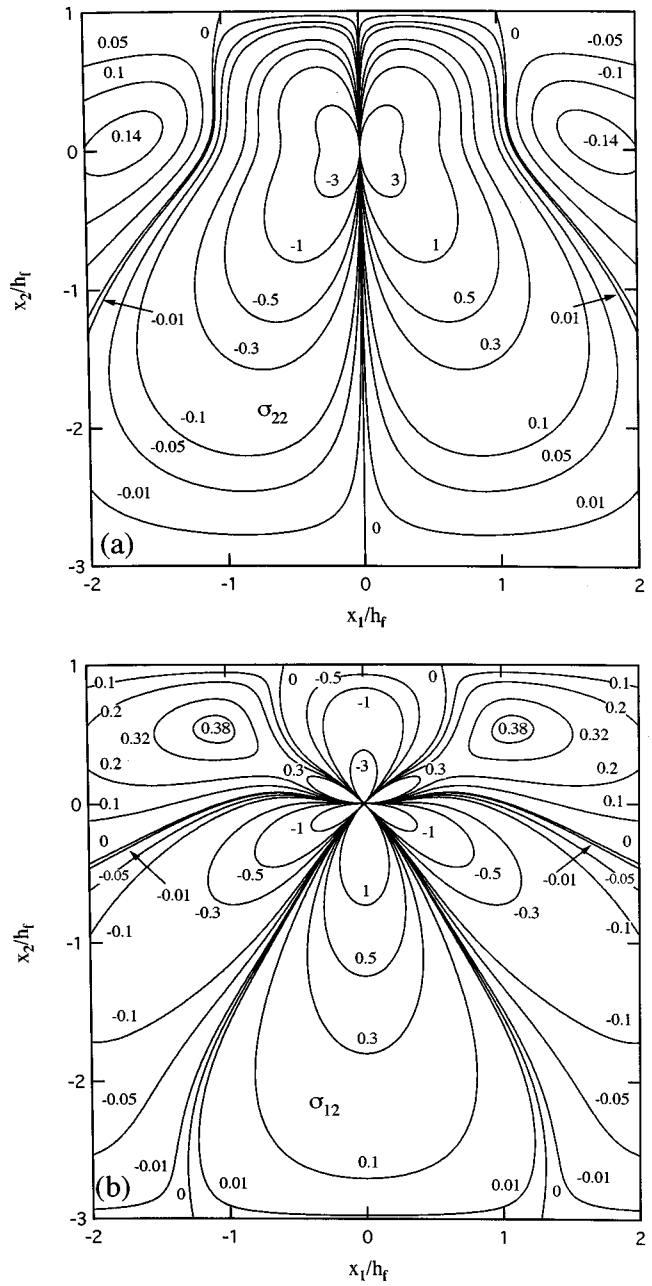

FIG. 3. Stress contours of an edge dislocation with Burgers vector $\mathbf{b}_2$ along the x_2 axis showing (a) σ_{22} and (b) σ_{12} where stresses are normalized by $\mu b_2/[2\pi(1-\nu)h_f]$.

60° dislocation and the screw dislocation lying in the $\langle 110\rangle$ direction.[27] The screw component of a dislocation does not release any mismatch stress. Therefore, the pure screw dislocation is not considered here. Only the 60° dislocation lying in the $\{111\}$ planes is studied hereafter. A thin film epitaxially deposited on the (010) plane of a substrate is considered in the present study. For a 60° dislocation lying in a $\{111\}$ plane, the dislocation line is along the $\langle 110\rangle$ direction and a possible Burgers vector in the coordinate system is $\mathbf{b}=b[1/2\ \overline{1}/\sqrt{2}\ 1/2]$. The radius of the dislocation core is taken as $r_0=b$. Using Eq. (10), the critical thickness of epilayer to form a dislocation as a function of substrate thickness and mismatch strain can be determined. The solid lines in Fig. 5 show the predicted mismatch strain magnitude $|\epsilon_m^0|$ as a function of the normalized critical epilayer thickness at different values of normalized substrate thickness, h_s/b. For a given substrate thickness, the mismatch strain increases with decreasing critical epilayer thickness. For the same critical epilayer thickness, the mismatch strain decreases with increasing substrate thickness. The dashed lines in Fig. 5 show the approximate solutions from Freund and Nix.[22] Since the present work is based on the ''FN'' model, as expected, the present result behaves in a similar way as the ''FN'' estimations, except that the present result tolerates a greater mismatch strain to reach the critical epilayer thickness for a given substrate thickness.

Downloaded 12 Mar 2002 to 128.219.47.178. Redistribution subject to AIP license or copyright, see http://ojps.aip.org/japo/japcr.jsp

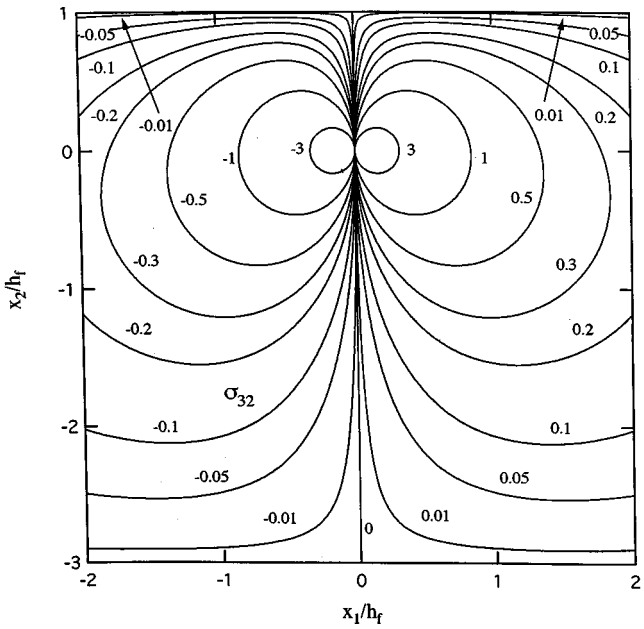

FIG. 4. Stress contours of a screw dislocation with Burgers vector $\mathbf{b}_3$ along the x_3 axis showing σ_{23} where stresses are normalized by $\mu b_3/[2\pi h_f]$.

IV. CONCLUSIONS

A mismatch dislocation at the interface between an epilayer and a substrate with a finite thickness is analyzed in the present study using the superposition principle and Fourier transformation. The stress field arising from the interface dislocation consists of four components: the stress field of the dislocation in an infinite domain, the stress fields of the two image dislocations due to the free surfaces of the epilayer and the substrate, and the stress field to remove the stresses arising from the former three dislocations on the free surfaces. The fourth stress field is obtained by Fourier transformation. The predicted stress contours are plotted to check the free-surface condition. Using the above stresses, the self-energy of dislocation, interaction energy between dislocation and free surface, and the lattice mismatch strain energy of both epilayer and substrate are obtained. The critical thickness of an epilayer to form a dislocation at the interface is calculated. The results show that for a given substrate thickness, the critical epilayer thickness decreases with increasing mismatch strain magnitude. For a given mismatch strain, the critical epilayer thickness decreases with increasing substrate thickness.

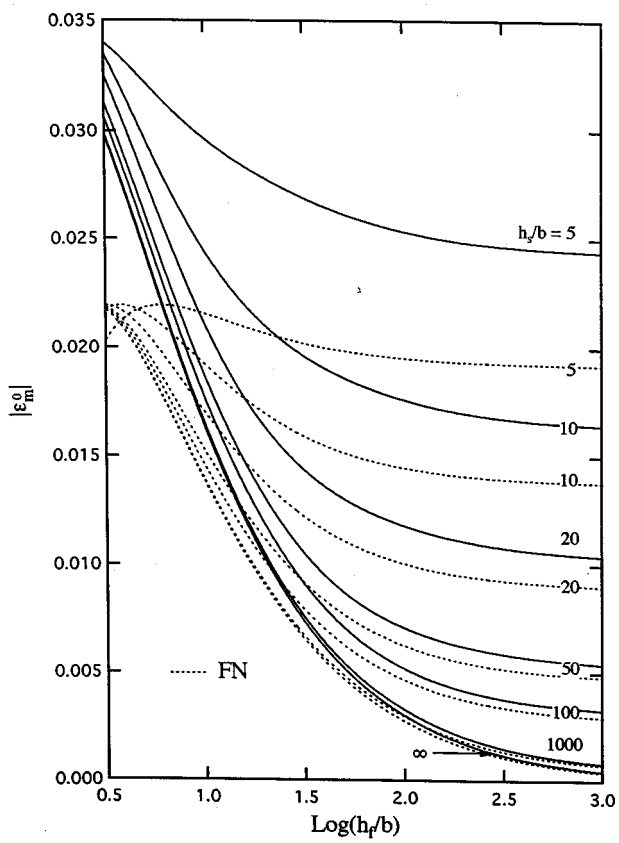

FIG. 5. Condition of critical epilayer thickness for relaxation of cubic crystals with a (100) interface by formation of 60° interface misfit dislocation through glide on a (111) plane ($\nu=0.25$).

ACKNOWLEDGMENTS

This work was financially supported by the Hong Kong Research Grants Council under RGC grant (TYZ), the National Science Council, Taiwan (SL), and the U.S. Department of Energy, Division of Materials Sciences, Office of Basic Energy Sciences, under Contract No. DE-AC05-96OR22464 with Lockheed Martin Energy Research Corp. (CHH).

APPENDIX A: EDGE DISLOCATION

In isotropic elasticity treatment, in-plane and antiplane elastic deformation can be studied separately. For the in-plane strain, two complex potentials $\phi(z)$ and $\omega(z)$ are used to represent the displacement and stress fields, such that

$$\begin{aligned}
&\sigma_{11}+\sigma_{22}=2[\phi'(z)+\overline{\phi'(z)}],\\
&\sigma_{22}-i\sigma_{12}=\phi'(z)+\overline{\omega'(z)}+(z-\overline{z})\overline{\phi''(z)},\\
&u(z)=u_1+iu_2=\frac{1}{2\mu}[\kappa\phi(z)-(z-\overline{z})\overline{\phi'(z)}-\overline{\omega(z)}],
\end{aligned}\tag{A1}$$

where $\kappa=3-4\nu$.

For an edge dislocation in an infinite domain [i.e., the first component in Eq. (4)], the complex potentials, $\phi^{(1)}$ and $\omega^{(1)}$, have the following forms:

$$\begin{aligned}
&\phi^{(1)}=B\ln(z),\quad \omega^{(1)}=\overline{B}\ln(z),\\
&B=\frac{\mu b_e}{i4\pi(1-\nu)},\quad b_e=b_1+ib_2.
\end{aligned}\tag{A2}$$

The second and third components of stress and displacement fields are derived from the traction-free condition along the epilayer and substrate surfaces, such that $\sigma^{(1)}+\sigma^{(2)}$ and $\sigma^{(1)}+\sigma^{(3)}$ satisfy the traction-free condition at $x_2=h_f$ and $x_2=-h_s$, respectively. The complex potentials of the second and third components are hence given by

Downloaded 12 Mar 2002 to 128.219.47.178. Redistribution subject to AIP license or copyright, see http://ojps.aip.org/japo/japcr.jsp

$$\phi^{(2)}=-B\ln(z-i2h_f)-\overline{B}\frac{z}{z-i2h_f},$$
$$\omega^{(2)}=-\overline{B}\ln(z-i2h_f)-B\frac{i2h_f}{z-i2h_f}+\overline{B}\frac{(i2h_f)^2}{(z-i2h_f)^2}. \tag{A3}$$

$$\phi^{(3)}=-B\ln(z+i2h_s)-\overline{B}\frac{z}{z+i2h_s},$$
$$\omega^{(3)}=-\overline{B}\ln(z+i2h_s)+B\frac{i2h_s}{z+i2h_s}+\overline{B}\frac{(i2h_s)^2}{(z+i2h_s)^2}. \tag{A4}$$

The fourth components of stress and displacement fields are formulated via the Fourier transformation. For simplicity, the superscript ''(4)'' will not be used hereafter unless it causes confusion. Following Willis *et al.*'s work,[7] the displacements and stresses in the ζ space are, respectively,

$$u_1=i\zeta[A_1e^{|\zeta|x_2}+A_2e^{-|\zeta|x_2}-A_3|\zeta|x_2e^{|\zeta|x_2}+A_4|\zeta|x_2e^{-|\zeta|x_2}],$$
$$u_2=|\zeta|[-A_1e^{|\zeta|x_2}+A_2e^{-|\zeta|x_2}+A_3(|\zeta|x_2-\kappa)e^{|\zeta|x_2}+A_4(|\zeta|x_2+\kappa)e^{-|\zeta|x_2}], \tag{A5}$$

and

$$\sigma_{11}=2\mu\zeta^2[A_1e^{|\zeta|x_2}+A_2e^{-|\zeta|x_2}-A_3(|\zeta|x_2-2\nu)e^{|\zeta|x_2}+A_4(|\zeta|x_2+2\nu)e^{-|\zeta|x_2}],$$
$$\sigma_{12}=2\mu i|\zeta|[A_1e^{|\zeta|x_2}-A_2e^{-|\zeta|x_2}-A_3(|\zeta|x_2-1+2\nu)e^{|\zeta|x_2}-A_4(|\zeta|x_2+1-2\nu)e^{-|\zeta|x_2}], \tag{A6}$$
$$\sigma_{22}=2\mu\zeta^2[-A_1e^{|\zeta|x_2}-A_2e^{-|\zeta|x_2}+A_3(|\zeta|x_2-2+2\nu)e^{|\zeta|x_2}-A_4(|\zeta|x_2+2-2\nu)e^{-|\zeta|x_2}].$$

The energy part associated with the fourth component of the in-plane stress field can be expressed in terms of ζ as

$$E_{0,4e}=-\frac{\mu}{\sqrt{2\pi}}\int_{-\infty}^{\infty}\Big\{(|\zeta|b_1+i\zeta b_2)A_1[a_1-1]-(|\zeta|b_1-i\zeta b_2)A_2\left[\frac{1}{a_1}-1\right]-(|\zeta|b_1+i\zeta b_2)\times A_3a_2a_1+\tfrac{1}{2}[(\kappa-1)|\zeta|b_1+(\kappa+1)i\zeta b_2]\times A_3[a_1-1]-(|\zeta|b_1-i\zeta b_2)A_4\frac{a_2}{a_1}-\tfrac{1}{2}[(\kappa-1)|\zeta|b_1-(\kappa+1)i\zeta b_2]A_4\left[\frac{1}{a_1}-1\right]\Big\}d\zeta. \tag{A7}$$

where $a_2=|\zeta|h_f$ and $a_1=\exp(a_2)$. Then the boundary conditions along the epilayer surface and the substrate surface may be re-written in the ζ space as follows: (a) traction free along the epilayer surface $x_2=h_f$, such that

$$-A_1a_1-A_2/a_1+A_3(a_2-2+2\nu)a_1-A_4(a_2+2-2\nu)/a_1+\frac{\sigma_{22}^{(3)}}{2\mu\zeta^2}=0,$$
$$A_1a_1-A_2/a_1-A_3(a_2-1+2\nu)a_1-A_4(a_2+1-2\nu)/a_1+\frac{\sigma_{12}^{(3)}}{2i\mu\zeta|\zeta|}=0, \tag{A8}$$

and (b) traction free along the substrate surface $x_2=-h_s$, such that

$$-A_1/a_3-A_2a_3+A_3(-a_4-2+2\nu)/a_3-A_4(-a_4+2-2\nu)\times a_3+\frac{\sigma_{22}^{(2)}}{2\mu\zeta^2}=0,$$
$$A_1/a_3-A_2a_3-A_3(-a_4-1+2\nu)/a_3-A_4(-a_4+1-2\nu)\times a_3+\frac{\sigma_{12}^{(2)}}{2i\mu\zeta|\zeta|}=0, \tag{A9}$$

where $a_4=|\zeta|h_s$ and $a_3=\exp(a_4)$.
Solutions of A_i $(i=1,2,3,4)$ from Eqs. (A8) and (A9) yield

$$A_1=\tfrac{1}{2}[A_3(2a_2-\kappa)-A_4/a_1^2+\Sigma_2^{(3)}/a_1],$$
$$A_2=-\tfrac{1}{2}[A_3a_1^2+A_4(2a_2+\kappa)-a_1\Sigma_1^{(3)}],$$
$$A_3=\langle 2(a_2+a_4)[\Sigma_2^{(2)}a_3-\Sigma_2^{(3)}/a_1]-[1/a_1^2-a_3^2]\times[\Sigma_1^{(2)}/a_3-a_1\Sigma_1^{(3)}]\rangle/D,$$
$$A_4=\langle[1/a_3^2-a_1^2][\Sigma_2^{(2)}a_3-\Sigma_2^{(3)}/a_1]-2(a_2+a_4)\times[\Sigma_1^{(2)}/a_3-a_1\Sigma_1^{(3)}]\rangle/D, \tag{A10}$$

where

$$D=4(a_2+a_4)^2-[a_1a_3-1/(a_1a_3)]^2,$$
$$\Sigma_1^{(2)}=\frac{\sigma_{22}^{(2)}}{2\mu\zeta^2}+\frac{\sigma_{12}^{(2)}}{i2\mu\zeta|\zeta|},\quad \Sigma_2^{(2)}=\frac{\sigma_{22}^{(2)}}{2\mu\zeta^2}-\frac{\sigma_{12}^{(2)}}{i2\mu\zeta|\zeta|},$$
$$\Sigma_1^{(3)}=\frac{\sigma_{22}^{(3)}}{2\mu\zeta^2}+\frac{\sigma_{12}^{(3)}}{i2\mu\zeta|\zeta|},\quad \Sigma_2^{(3)}=\frac{\sigma_{22}^{(3)}}{2\mu\zeta^2}-\frac{\sigma_{12}^{(3)}}{i2\mu\zeta|\zeta|}. \tag{A11}$$

From Eqs. (A1) and (A3) the second component of traction along the substrate surface is

$$\sigma_{22}^{(2)}=-\frac{(B+\overline{B})x_1}{x_1^2+(h_s+2h_f)^2}-\frac{2(B+\overline{B})(h_s+2h_f)^2x_1}{[x_1^2+(h_s+2h_f)^2]^2}+\frac{i(B-\overline{B})h_s[x_1^2-(h_s+2h_f)^2]}{[x_1^2+(h_s+2h_f)^2]^2}+\frac{4(B+\overline{B})[h_sh_f+h_f^2][x_1^3-3x_1(h_s+2h_f)^2]}{[x_1^2+(h_s+2h_f)^2]^3}-\frac{4i(B-\overline{B})[h_sh_f+h_f^2][h_s+2h_f][3x_i^2-(h_s+2h_f)^2]}{[x_1^2+(h_s+2h_f)^2]^3}, \tag{A12}$$

Downloaded 12 Mar 2002 to 128.219.47.178. Redistribution subject to AIP license or copyright, see http://ojps.aip.org/japo/japcr.jsp

$$\sigma_{12}^{(2)}=-\frac{i(B-\overline{B})x_1}{x_1^2+(h_s+2h_f)^2}+\frac{2i(B-\overline{B})(h_s+2h_f)^2x_1}{[x_1^2+(h_s+2h_f)^2]^2}+\frac{(B+\overline{B})h_s[x_1^2-(h_s+2h_f)^2]}{[x_1^2+(h_s+2h_f)^2]^2}+\frac{4i(B-\overline{B})[h_sh_f+h_f^2][x_1^3-3x_1(h_s+2h_f)^2]}{[x_1^2+(h_s+2h_f)^2]^3}+\frac{4(B+\overline{B})[h_sh_f+h_f^2][h_s+2h_f][3x_1^2-(h_s+2h_f)^2]}{[x_1^2+(h_s+2h_f)^2]^3}.$$

Also, from Eqs. (A1) and (A4), the third component of traction along the epilayer surface is

$$\sigma_{22}^{(3)}=-\frac{(B+\overline{B})x_1}{x_1^2+(h_f+2h_s)^2}-\frac{2(B+\overline{B})(h_f+2h_s)^2x_1}{[x_1^2+(h_f+2h_s)^2]^2}-\frac{i(B-\overline{B})h_f[x_1^2-(h_f+2h_s)^2]}{[x_1^2+(h_f+2h_s)^2]^2}+\frac{4(B+\overline{B})[h_sh_f+h_s^2][x_1^3-3x_1(h_f+2h_s)^2]}{[x_1^2+(h_f+2h_s)^2]^3}+\frac{4i(B-\overline{B})[h_sh_f+h_s^2][h_f+2h_s][3x_1^2-(h_f+2h_s)^2]}{[x_1^2+(h_f+2h_s)^2]^3},$$

$$\sigma_{12}^{(3)}=-\frac{i(B-\overline{B})x_1}{x_1^2+(h_f+2h_s)^2}+\frac{2i(B-\overline{B})(h_f+2h_s)^2x_1}{[x_1^2+(h_f+2h_s)^2]^2}-\frac{(B+\overline{B})h_f[x_1^2-(h_f+2h_s)^2]}{[x_1^2+(h_f+2h_s)^2]^2}+\frac{4i(B-\overline{B})[h_sh_f+h_s^2][x_1^3-3x_1(h_f+2h_s)^2]}{[x_1^2+(h_f+2h_s)^2]^3}-\frac{4(B+\overline{B})[h_sh_f+h_s^2][h_f+2h_s][3x_1^2-(h_f+2h_s)^2]}{[x_1^2+(h_f+2h_s)^2]^3}. \tag{A13}$$

Using the Fourier transformations

$$\frac{1}{x_1^2+4h^2}\Rightarrow\sqrt{\frac{\pi}{2}}\frac{1}{2ha_1^2},\quad \frac{x_1}{(x_1^2+4h^2)}\Rightarrow\sqrt{\frac{\pi}{2}}\frac{i|\zeta|}{\zeta a_1^2},$$
$$\frac{4h^2-x_1^2}{(x_1^2+4h^2)^2}\Rightarrow\sqrt{\frac{\pi}{2}}\frac{|\zeta|}{a_1^2},\quad \frac{x_1}{(x_1^2+4h^2)^2}\Rightarrow\sqrt{\frac{\pi}{2}}\frac{i\zeta}{4ha_1^2}, \tag{A14}$$
$$\frac{4h^2-3x_1^2}{(x_1^2+4h^2)^3}\Rightarrow\sqrt{\frac{\pi}{2}}\frac{\zeta^2}{4ha_1^2},\quad \frac{x_1(12h^2-x_1^2)}{(x_1^2+4h^2)^3}\Rightarrow\sqrt{\frac{\pi}{2}}\frac{i\zeta|\zeta|}{2a_1^2},$$

the traction in Eqs. (A12) and (A13) can be transferred into the ζ space, such that

$$\begin{aligned}\sigma_{22}^{(2)}&=-i\sqrt{\pi/2}\exp[-|\zeta|(h_s+2h_f)][(B+\overline{B})|\zeta|/\zeta+(B+\overline{B})(h_s+2h_f)\zeta+(B-\overline{B})h_s|\zeta|+2(B+\overline{B})\times[h_sh_f+h_f^2]\zeta|\zeta|-2(B-\overline{B})[h_sh_f+h_f^2]\zeta^2],\\ \sigma_{12}^{(2)}&=\sqrt{\pi/2}\exp[-|\zeta|(h_s+2h_f)][(B-\overline{B})|\zeta|/\zeta-(B-\overline{B})(h_s+2h_f)\zeta-(B+\overline{B})h_s|\zeta|+2(B-\overline{B})\times[h_sh_f+h_f^2]\zeta|\zeta|-2(B+\overline{B})[h_sh_f+h_f^2]\zeta^2],\\ \sigma_{22}^{(3)}&=-i\sqrt{\pi/2}\exp[-|\zeta|(h_f+2h_s)][(B+\overline{B})|\zeta|/\zeta+(B+\overline{B})(h_f+2h_s)\zeta-(B-\overline{B})h_f|\zeta|+2(B+\overline{B})\times[h_sh_f+h_s^2]\zeta|\zeta|+2(B-\overline{B})[h_sh_f+h_s^2]\zeta^2],\\ \sigma_{12}^{(3)}&=\sqrt{\pi/2}\exp[-|\zeta|(h_f+2h_s)][(B-\overline{B})|\zeta|/\zeta-(B-\overline{B})(h_f+2h_s)\zeta+(B+\overline{B})h_f|\zeta|+2(B-\overline{B})\times[h_sh_f+h_s^2]\zeta|\zeta|+2(B+\overline{B})[h_sh_f+h_s^2]\zeta^2].\end{aligned} \tag{A15}$$

Note that

$$B+\overline{B}=2Cb_2,\quad B-\overline{B}=-i2Cb_1,\quad \text{and } C=\frac{\mu}{4\pi(1-\nu)}. \tag{A16}$$

APPENDIX B: SCREW DISLOCATION

For an antiplane strain, the displacement u_3 can be expressed as an imaginary part of an arbitrary analytic function, $g(z)$, such that

$$u_3=\frac{1}{\mu}\mathrm{Im}[g(z)], \tag{B1}$$

where Im denotes the imaginary part of a complex function, and $z=x_1+ix_2$. The stress components σ_{31} and σ_{32} can be obtained by differentiating the complex potential, g, with respect to z, such that

$$\sigma=\sigma_{32}+i\sigma_{31}=[g(z)]', \tag{B2}$$

where the prime stands for the differentiation.

For a screw dislocation located in an infinite domain [the first component in Eq. (4)], the complex potential and the corresponding stress are given by

$$g^{(1)}=\frac{\mu b_3}{2\pi}\ln(z),\quad \sigma^{(1)}=\frac{\mu b_3}{2\pi z}. \tag{B3}$$

In order to meet the traction-free condition on the epilayer surface and substrate surface, the complex potential and the corresponding stress for the second and third components of stress field are given by

$$g^{(2)}=-\frac{\mu b_3}{2\pi}\ln(z-i2h_f),\quad \sigma^{(2)}=-\frac{\mu b_3}{2\pi(z-i2h_f)}, \tag{B4}$$

$$g^{(3)}=-\frac{\mu b_3}{2\pi}\ln(z+i2h_s),\quad \sigma^{(3)}=-\frac{\mu b_3}{2\pi(z+i2h_s)}. \tag{B5}$$

Using the same approach for the edge dislocation in Appendix I, the fourth component of the stress and displacement fields for a screw dislocation can be derived, and the general solution for u_3 is

$$u_3=B_1e^{|\zeta|x_2}+B_2e^{-|\zeta|x_2}, \tag{B6}$$

Downloaded 12 Mar 2002 to 128.219.47.178. Redistribution subject to AIP license or copyright, see http://ojps.aip.org/japo/japcr.jsp

where B_1 and B_2 are constants to be determined from the boundary conditions.

The traction free condition at $x_2=h_f$ and $x_2=-h_s$ requires

$$\mu|\zeta|(B_1a_1-B_2/a_1)+\sigma_{32}^{(3)}=0, \tag{B7}$$

$$\mu|\zeta|(B_1/a_3-B_2a_3)+\sigma_{32}^{(2)}=0. \tag{B8}$$

Calculating the stress components and solving Eqs. (B7) and (B8) lead to

$$B_1=\frac{b_3}{2\sqrt{2\pi}}\frac{i}{\zeta}\frac{1-1/a_1^2}{a_1^2a_3^2-1},\quad B_2=-\frac{b_3}{2\sqrt{2\pi}}\frac{i}{\zeta}\frac{1-1/a_3^2}{a_1^2a_3^2-1}. \tag{B9}$$

The stress component $\sigma_{31}^{(4)}$ and the associate energy are given by

$$\sigma_{31}^{(4)}=-i\mu\zeta(B_1e^{|\zeta|x_2}+B_2e^{-|\zeta|x_2}) \tag{B10}$$

$$\begin{aligned}
E_{0,4s}&=-\frac{\mu b_3^2}{8\pi}\int_{-\infty}^{\infty}\frac{1}{|\zeta|}\frac{a_1+1/a_1^2-1/(a_1a_3^2)+1/a_3^2-2}{a_1^2a_3^2-1}d\zeta\\
&=-\frac{\mu b_3^2}{4\pi}\sum_{n=0}^{\infty}\ln\frac{[2n(h_s+h_f)+2h_s+h_f][2n(h_s+h_f)+2h_s+4h_f][2n(h_s+h_f)+4h_s+2h_f]}{[2n(h_s+h_f)+4h_s+3h_f][2(n+1)(h_s+h_f)]^2}\\
&=-\frac{\mu b_3^2}{4\pi}\ln(2h_s+h_f)-\frac{\mu b_3^2}{4\pi}\sum_{n=0}^{\infty}\ln\frac{n(n+3)(h_s+h_f)^2+(2h_s+h_f)(h_s+2h_f)}{[(n+1)(h_s+h_f)]^2}\\
&=\frac{\mu b_3^2}{4\pi}\ln\left\{\frac{(h_s+h_f)(h_s+2h_f)}{2\pi h_sh_f}\cos\left[\frac{\pi(h_f-h_s)}{2(h_s+h_f)}\right]\right\}.
\end{aligned} \tag{B11}$$

[1] F. C. Frank and J. H. van der Merwe, Proc. R. Soc. London, Ser. **198**, 205 (1949); **198**, 216 (1949); **200**, 125 (1949).
[2] J. W. Mattews, Philos. Mag. **23**, 1405 (1971).
[3] J. W. Mathews and A. E. Blakeslee, J. Cryst. Growth **27**, 118 (1974).
[4] J. W. Matthews, J. Vac. Sci. Technol. **12**, 126 (1975).
[5] L. B. Freund, J. Mech. Phys. Solids **38**, 657 (1990).
[6] L. B. Freund, Scr. Metall. Mater. **27**, 669 (1992).
[7] J. R. Willis, S. C. Jain, and R. Bullough, Philos. Mag. A **62**, 115 (1990).
[8] J. R. Willis, S. C. Jain, and R. Bullough, Philos. Mag. A **64**, 629 (1991).
[9] S. C. Jain, T. J. Gosling, J. R. Willis, D. H. J. Totterdell, and R. Bullough, Philos. Mag. A **65**, 1151 (1992).
[10] T. J. Gosling, S. C. Jain, J. R. Willis, A. Atkinson, and R. Bullough, Philos. Mag. A **66**, 119 (1992).
[11] T. J. Gosling, J. R. Willis, and R. Bullough, and S. C. Jain, J. Appl. Phys. **73**, 8297 (1993).
[12] T. J. Gosling and J. R. Willis, Philos. Mag. A **69**, 65 (1994).
[13] W. A. Jesser and J. H. van der Merwe, in *Dislocations in Solids*, edited by F. R. N. Nabarro (Elsevier Science, Amsterdam, 1989), Vol. 8, Chap. 41, p. 421.
[14] L. B. Freund, Adv. Appl. Mech. **30**, 1 (1993).
[15] T.-Y. Zhang, J. E. Hack, and L. J. Guido, J. Appl. Phys. **75**, 2358 (1994).
[16] T.-Y. Zhang, J. E. Hack, and L. J. Guido, J. Appl. Phys. **75**, 2363 (1994).
[17] T.-Y. Zhang, Phys. Status Solidi A **148**, 175 (1995).
[18] T.-Y. Zhang, Phys. Status Solidi A **152**, 415 (1995).
[19] T.-Y. Zhang, J. Appl. Phys. **78**, 4948 (1995).
[20] T.-Y. Zhang, Defect Diffus. Forum **136–137**, 61 (1996).
[21] S. C. Jain, A. H. Harker, and R. A. Cowley, Philos. Mag. A **75**, 1461 (1997).
[22] L. B. Freund and W. D. Nix, Appl. Phys. Lett. **69**, 173 (1996).
[23] Y. H. Lo, Appl. Phys. Lett. **59**, 2311 (1991).
[24] A. R. Powell, S. S. Iyer, and F. K. LeGoues, Appl. Phys. Lett. **64**, 1856 (1994).
[25] F. J. Guarin, S. S. Iyer, Z. Yang, and W. I. Wang, Proceedings of the 3rd International Symposium on Wafer Bonding Physics Applications, 1995, Vol. 95–97, p. 561.
[26] J. D. Eshelby, in *Dislocation in Solids*, edited by F. R. N. Narbarro (Elsevier Science, Amsterdam, 1979), Vol. 1, Chap. 3, p. 167.
[27] H. Alexander, in *Dislocations in Solids*, edited by F. R. N. Nabarro (Elsevier Science, Amsterdam, 1986), Vol. 7, Chap. 35.

Downloaded 12 Mar 2002 to 128.219.47.178. Redistribution subject to AIP license or copyright, see http://ojps.aip.org/japo/japcr.jsp